JAERI-M
89-138

MONTE CARLO SIMULATION FOR THE CALIBRATION OF NEUTRON SOURCE STRENGTH MEASUREMENT OF JT-60 UPGRADE

October 1989

Takeo NISHITANI

日本原子力研究所
Japan Atomic Energy Research Institute

JAERI-Mレポートは，日本原子力研究所が不定期に公刊している研究報告書です。
入手の問合わせは，日本原子力研究所技術情報部情報資料課（〒319-11茨城県那珂郡東海村）あて，お申しこしください。なお，このほかに財団法人原子力弘済会資料センター（〒319-11 茨城県那珂郡東海村日本原子力研究所内）で複写による実費頒布をおこなっております。

JAERI-M reports are issued irregularly.
Inquiries about availability of the reports should be addressed to Information Division Department of Technical Information, Japan Atomic Energy Research Institute, Tokai-mura, Naka-gun, Ibaraki-ken 319-11, Japan.

編集兼発行　日本原子力研究所
印　　刷　㈱高野高速印刷

JAERI-M 89-138

Monte Carlo Simulation for the Calibration of Neutron Source Strength Measurement of JT-60 Upgrade

Takeo NISHITANI

Department of Large Tokamak Research
Naka Fusion Research Establishment
Japan Atomic Energy Research Institute
Naka-machi, Naka-gun, Ibaraki-ken

(Received September 8, 1989)

The calibration of the relation between the neutron source strength in the whole plasma and the output of neutron monitor is important to evaluate the fusion gain in tokamaks with DD or DT operation. JT-60 will be modified to be tokamak of deuterium plasma with Ip≤7MA and V≤110 m^3. The source strength of JT-60 Upgrade will be measured with ^{235}U and ^{238}U fission fission chambers. Detection efficiencies for source neutron are calculated by the Monte Carlo code MCNP with 3-dimensional modelling of JT-60 upgrade and with the poloidally distributed neutron source. More than 90% of fission chamber's counts are contributed by source of $-85°<\theta<85°$ in the toroidal angle. The uncertainties of the detection efficiencies due to plasma parameter varieties are ±11% and ±8% for ^{235}U and ^{238}U detectors, respectively. Detection efficiencies are sensitive to major radius of the detector position, but not so sensitive to vertical and toroidal shift of the detector positions. And total uncertainties combined detector position errors are ±13% and ±9% for ^{235}U and ^{238}U detectors, respectively. The modelling errors of the detection efficiencies are so large for the ^{238}U detector that more precise modelling including the port boxes is needed.

Keywords: Neutron Source Strength Calibration, JT-60 Upgrade, Monte Carlo Simulation, MCNP, Fission Chamber, Deuterium Plasma, Neutron Diagnostics

大電流化ＪＴ－６０における中性子発生量測定の較正のためのモンテカルロ計算

日本原子力研究所那珂研究所臨界プラズマ研究部
西谷　健夫

（１９８９年９月８日受理）

ＤＤまたはＤＴ運転を行うトカマク装置において，プラズマ全体から発生した中性子の量と中性子モニターの出力値との関係を較正することは，核融合利得を評価する上で重要である。ＪＴ－６０は大電流化改造後，最大プラズマ電流７ＭＡ，最大プラズマ体積１１０㎥の重水素トカマク装置となるが，その中性子発生量は^{235}Ｕおよび^{238}Ｕの核分裂計算管で測定することを予定している。そこで大電流化ＪＴ－６０の３次元形状モデルおよびポロイダル分布を考慮した中性子発生源を用いた中性子モンテカルロコードＭＣＮＰによって，それらの核分裂計数管の発生中性子に対する検出効率の計算を行った。核分裂計数管の出力９０％以上は，トロイダル角にして－８５°から８５°の範囲の中性子が寄与することがわかった。また，プラズマパラメータによる^{235}Ｕおよび^{238}Ｕの核分裂計数管の発生中性子に対する検出効率の不確定性は，それぞれ±１１％，±８％であり，検出効率は検出器位置の大半径方向に敏感であるが，垂直方向およびトロイダル方向にはまり影響されない。プラズマパラメータおよび検出器位置による不確定性を総合すると^{235}Ｕおよび^{238}Ｕの核分裂計数管に対し，それぞれ±１３％，±９％であった。本計算におけるモデル化の誤差は^{238}Ｕ核分裂計数管に対して大きく，ポートボックスのモデル化を含んださらに詳し計算が必要と思われる。

那珂研究所：〒310－01　茨城県那珂郡那珂町大字向山８０１－１

Contents

目　　次

1. INTRODUCTION

Neutron production rate is one of the most important parameter in the DD or DT operational fusion device indication fusion gain directly. The calibration of the relation between the neutron source strength in the whole plasma and the output of neutron monitor is a most important problem in the measurements of the neutron production rate. The calibration is rather difficult because the neutron source is distributed in the plasma which is surrounded with many complicated structures such as first wall, vacuum vessel poloidal and toroidal coils. Many efforts and time are devoted to the calibration at many tokamaks [1-8]

The output of a neutron detector is given by

$$C = S_0 \int S(r,\theta,\phi)\, G(r,\theta,\phi) dV \qquad (1)$$

where C is the detector output, S_0 is the neutron source strength, $S(r,\theta,\phi)$ is source profile at minor radius of r, toroidal angle of θ and poloidal angle of ϕ whose volume integral of the whole plasma is normalized to be unity, and $G(r,\theta,\phi)$ is the detector response to the point source. In general the detector response function $G(r,\theta,\phi)$ is estimated by the point neutron source set at the various points in the vacuum vessel. In TFTR [1-4] the calibration has been performed by using a ^{252}Cf neutron source, a DD neutron generator, and a DT neutron generator. JET [5,6] has employed the calibration using ^{252}Cf neutron source. Because the calibration takes long time to get sufficient counts of the detector, the number of the mapping point is limited to be not more than several tens . Usually $G(r,\theta,\phi)$ is estimated only on the magnetic axis in order to save the calibration time where the source neutron is assumed to be generated on the magnetic axis. On large tokamaks some source points opposite side of the detector in the vacuum vessel are so far from the detector that an intense neutron source or neutron generator is required for the calibration. Whereas the simulation calculation of the neutron transport considering the the source distribution can estimate directly the integral term in Eq. (1) which is the detection efficiency.

JT-60 will be modified to be tokamak of deuterium plasma with Ip≤7MA and V≤100m^3, which is called JT-60 Upgrade (JT-60U) [9]. The neutron source strength of JT-60 Upgrade will be measured with ^{235}U and ^{238}U fission chambers mainly . The Monte Carlo code MCNP [10,11] with 3-dimensional

modelling of JT-60 upgrade and with poloidally distributed neutron source is provided to estimate the uncertainty of the detection efficiencies due to plasma parameters and the detector position dependence.

Section 2 and Section 3 describe tokamak parameters and neutron measurements plan of JT-60 Upgrade, respectively. Section 4 describes the calculation procedures, Section 5 presents the results of the calculation. The modelling errors of the calculation are discussed in Section 6. The conclusions are given in Section 7.

2. JT-60 Upgrade

JT-60 will be modified by complete replacing of vacuum vessel and poloidal coils to be DD operational tokamak characterized by the single null D-shaped divertor configuration. The machine and operational parameters are summarized in Table 1. The major and minor radii are approximately 3.4m and 1.1m, respectively. The maximum plasma current is 6MA in the divertor configuration and 7MA in the limiter configuration. The additionally heating is 40MW of deuterium NB injection, 15MW of LHRF,and 10MW of ICRF. More than 10MW of NB injection with 500keV negative ion source is proposed. Standard operational gas is a deuterium and the maximum neutron yield of 2×10^{17}n/s is expected in the full power discharge

JT-60U has three typical configurations as shown in Fig. 1. In the limiter configuration, 7MA limited plasma can be produced with ellipticity of 1.40. and plasma volume of 107 m^3. In the standard divertor configuration 6MA diverted plasma can be produced with ellipticity of 1.52 and plasma volume of 91 m^3. In the elongated divertor configuration 6MA diverted plasma can be produced with ellipticity of 1.76 and the plasma volume of 76 m^3.

3. PLAN OF NEUTRON DIAGNOSTICS AND NEUTRON SOURCE STRENGTH CALIBRATION

3.1 PLAN OF NEUTRON DIAGNOSTICS

The neutron diagnostics plan of JT-60U is summarized in Table 2. The time evolution of neutron source strength will be measured with ^{235}U and ^{238}U fission chambers installed at three point around the vacuum vessel. The shot integrated neutron strength will be measured with the activation foil method by using a pneumatic tube system. Precise neutron spectrum of the

modelling of JT-60 upgrade and with poloidally distributed neutron source is provided to estimate the uncertainty of the detection efficiencies due to plasma parameters and the detector position dependence.

Section 2 and Section 3 describe tokamak parameters and neutron measurements plan of JT-60 Upgrade, respectively. Section 4 describes the calculation procedures, Section 5 presents the results of the calculation. The modelling errors of the calculation are discussed in Section 6. The conclusions are given in Section 7.

2. JT-60 Upgrade

JT-60 will be modified by complete replacing of vacuum vessel and poloidal coils to be DD operational tokamak characterized by the single null D-shaped divertor configuration. The machine and operational parameters are summarized in Table 1. The major and minor radii are approximately 3.4m and 1.1m, respectively. The maximum plasma current is 6MA in the divertor configuration and 7MA in the limiter configuration. The additionally heating is 40MW of deuterium NB injection, 15MW of LHRF,and 10MW of ICRF. More than 10MW of NB injection with 500keV negative ion source is proposed. Standard operational gas is a deuterium and the maximum neutron yield of 2×10^{17}n/s is expected in the full power discharge

JT-60U has three typical configurations as shown in Fig. 1. In the limiter configuration, 7MA limited plasma can be produced with ellipticity of 1.40. and plasma volume of 107 m^3. In the standard divertor configuration 6MA diverted plasma can be produced with ellipticity of 1.52 and plasma volume of 91 m^3. In the elongated divertor configuration 6MA diverted plasma can be produced with ellipticity of 1.76 and the plasma volume of 76 m^3.

3. PLAN OF NEUTRON DIAGNOSTICS AND NEUTRON SOURCE STRENGTH CALIBRATION

3.1 PLAN OF NEUTRON DIAGNOSTICS

The neutron diagnostics plan of JT-60U is summarized in Table 2. The time evolution of neutron source strength will be measured with ^{235}U and ^{238}U fission chambers installed at three point around the vacuum vessel. The shot integrated neutron strength will be measured with the activation foil method by using a pneumatic tube system. Precise neutron spectrum of the

modelling of JT-60 upgrade and with poloidally distributed neutron source is provided to estimate the uncertainty of the detection efficiencies due to plasma parameters and the detector position dependence.

Section 2 and Section 3 describe tokamak parameters and neutron measurements plan of JT-60 Upgrade, respectively. Section 4 describes the calculation procedures, Section 5 presents the results of the calculation. The modelling errors of the calculation are discussed in Section 6. The conclusions are given in Section 7.

2. JT-60 Upgrade

JT-60 will be modified by complete replacing of vacuum vessel and poloidal coils to be DD operational tokamak characterized by the single null D-shaped divertor configuration. The machine and operational parameters are summarized in Table 1. The major and minor radii are approximately 3.4m and 1.1m, respectively. The maximum plasma current is 6MA in the divertor configuration and 7MA in the limiter configuration. The additionally heating is 40MW of deuterium NB injection, 15MW of LHRF,and 10MW of ICRF. More than 10MW of NB injection with 500keV negative ion source is proposed. Standard operational gas is a deuterium and the maximum neutron yield of 2×10^{17}n/s is expected in the full power discharge

JT-60U has three typical configurations as shown in Fig. 1. In the limiter configuration, 7MA limited plasma can be produced with ellipticity of 1.40. and plasma volume of 107 m^3. In the standard divertor configuration 6MA diverted plasma can be produced with ellipticity of 1.52 and plasma volume of 91 m^3. In the elongated divertor configuration 6MA diverted plasma can be produced with ellipticity of 1.76 and the plasma volume of 76 m^3.

3. PLAN OF NEUTRON DIAGNOSTICS AND NEUTRON SOURCE STRENGTH CALIBRATION

3.1 PLAN OF NEUTRON DIAGNOSTICS

The neutron diagnostics plan of JT-60U is summarized in Table 2. The time evolution of neutron source strength will be measured with ^{235}U and ^{238}U fission chambers installed at three point around the vacuum vessel. The shot integrated neutron strength will be measured with the activation foil method by using a pneumatic tube system. Precise neutron spectrum of the

DD neutron will be measure by ^{3}He ionization chamber [12,13] for the ion temperature measurement in OH or ICRF experiments. The overall energy spectrum in the rage of energy from 1.5 to 14MeV will be measured by NE213 scintillation detector [14] with the energy resolution of 10% by which the triton burn-up ratio can be estimated. The neutron multi-collimator system consisting of about 10 channel detectors is proposed to measure the source profile of the DD neutrons.

3.2 FISSION CHAMBERS

Fission chambers are most important diagnostics in the neutron source strength measurement. Fission chamber is a ionization chamber of which wall is coated by fissile material such as ^{235}U and ^{238}U. Energy released by fission is so large, 150-200MeV, that it is easy to reject the effect of γ-ray whose energy is not more than 20MeV in the DD operational tokamaks. The mean free path of the fission fragment is so short that distance between the anode and cathode can be much shorter than that of other gas counter such as BF_3 chamber. Therefor fission chambers are not so affected by the magnetic field.

We have a plan that the ^{235}U detector will be used in the low neutron yield discharges and the ^{238}U detector will be used in the high neutron yield discharges such as high-power NB heating experiments. The detail of the fission chambers have not been fixed yet. The counting sensitivity is required to be 0.1 to 0.5 cps/nv for the ^{235}U detector and 1 to 5×10^{-4} cps/nv for the ^{238}U detector. 0.4-1g of ^{235}U and about 1g of ^{238}U are required as fissile material in the ^{235}U and ^{238}U detectors, respectively. The fission chambers are used in the pulse counting mode within the counting rate of 10^3-10^6cps. For the counting rate larger than 10^6cps, the campbelling mode [15] will be employed.

Figure 2 shows the example design of the fission chambers. The ^{235}U detector is surrounded by 50mm thick lead of γ-ray shield, 50mm thick polyethylene of moderator, and 1mm thick cadmium of thermal neutron shield whose neutron sensitivity is estimated to be almost constant in the energy range of 0.55eV to 2.5MeV. The ^{238}U detector is surrounded by 50mm thick lead of gamma shield only.

Three pairs of ^{235}U and ^{238}U fission chambers will be installed near the vacuum vessel on the midplane as shown in Fig. 3. The ^{235}U detector will be mounted behind the ^{238}U detector because the ^{238}U detector is sensitive to the direct and one or two times scattered DD neutrons.

3.3 PLAN OF NEUTRON SOURCE STRENGH CALIBRATION

Figure 4 shows the diagram of the neutron calibration plan on JT-60U. Neutron yield of 10^{10} to 10^{17} n/s and.the total neutron flux of 10^{4} to 10^{11} at the detector position are expected in JT-60U. We have two plans of the neutron calibration.

One is a point source calibration using a neutron source whose neuron yield is 5×10^{7} n/s. The detector response to the point source will be measured by the neutron source inserted on the magnetic axis in the vacuum vessel. The counting rate of 10 to 100 cps is expected for ^{235}U detector. It will take long time to get sufficient counts when the neutron source is set far from the detector. The ^{238}U detector will be cross-calibrated by the ^{235}U detector in the DD discharge experiments.

Another is the calibration calculation using Monte Carlo code MCNP with 3-dimesional modelling of tokamak device and toroidal neutron source with poloidally distribution. MCNP calculates the detection efficiency of each detector for source neutron can be obtained by multiplying the detector sensitivity by the neutron flux at the detector calculated by the MCNP. The calculated neutron flux has larger statistical error at lower energy. The ^{235}U detector has a large sensitivity to low energy neutrons. Therefor it seemed that calculated efficiency of the ^{235}U detector has larger ambiguity than that of the ^{238}U detector.

4. CALCULATION

The calculation code is MCNP ver.3 with the original neutron cross-section set based on ENDF/B-IV mainly. The neutron source in the calculation is 2.45MeV monoenergetic and isotropic. The 14MeV neutron (DT component) is neglected in the calculation. The source distribution is a point source for the simulation of the point source calibration and a toroidally symmetric source for the direct calculation of the detection efficiencies. The toroidal source has a poloidal distribution as follows;

$$S = \left[1 - \left\{ \frac{(R-R_P)^2}{a_p^2} + \frac{(Z-Z_P)^2}{a_p^2 \kappa^2} \right\} \right]^m \qquad (2)$$

where R_P is a major radius, a_P is a minor radius, Z_P is a vertical shift of the plasma center, κ is a ellipticity, and m is a index of parabolic profile. Because

3.3 PLAN OF NEUTRON SOURCE STRENGH CALIBRATION

Figure 4 shows the diagram of the neutron calibration plan on JT-60U. Neutron yield of 10^{10} to 10^{17} n/s and.the total neutron flux of 10^{4} to 10^{11} at the detector position are expected in JT-60U. We have two plans of the neutron calibration.

One is a point source calibration using a neutron source whose neuron yield is 5×10^{7} n/s. The detector response to the point source will be measured by the neutron source inserted on the magnetic axis in the vacuum vessel. The counting rate of 10 to 100 cps is expected for ^{235}U detector. It will take long time to get sufficient counts when the neutron source is set far from the detector. The ^{238}U detector will be cross-calibrated by the ^{235}U detector in the DD discharge experiments.

Another is the calibration calculation using Monte Carlo code MCNP with 3-dimesional modelling of tokamak device and toroidal neutron source with poloidally distribution. MCNP calculates the detection efficiency of each detector for source neutron can be obtained by multiplying the detector sensitivity by the neutron flux at the detector calculated by the MCNP. The calculated neutron flux has larger statistical error at lower energy. The ^{235}U detector has a large sensitivity to low energy neutrons. Therefor it seemed that calculated efficiency of the ^{235}U detector has larger ambiguity than that of the ^{238}U detector.

4. CALCULATION

The calculation code is MCNP ver.3 with the original neutron cross-section set based on ENDF/B-IV mainly. The neutron source in the calculation is 2.45MeV monoenergetic and isotropic. The 14MeV neutron (DT component) is neglected in the calculation. The source distribution is a point source for the simulation of the point source calibration and a toroidally symmetric source for the direct calculation of the detection efficiencies. The toroidal source has a poloidal distribution as follows;

$$S = \left[1 - \left\{ \frac{(R-R_P)^2}{a_P^2} + \frac{(Z-Z_P)^2}{a_P^2 \kappa^2} \right\} \right]^m \qquad (2)$$

where R_P is a major radius, a_P is a minor radius, Z_P is a vertical shift of the plasma center, κ is a ellipticity, and m is a index of parabolic profile. Because

the original MCNP code can not treat the toroidal source with the poloidal profile, the distributed source routine for the MORCE code are employed to be linked to the MCNP code. By using the distributed source routine, the plasma parameter dependence of the detection efficiency can be estimated. Standard parameters in the calculation are R_P=3.4m, a_P=0.98m, Z_P=0.16m, κ=1.5, and m=2, which are parameters of the standard divertor configuration.

The lower cut off energy of the calculation is 0.55eV which is a cadmium cutoff energy. The energy bin in the calculation is presented in Table 3. The sensitivities of the detectors to neutrons depend on the fission cross-section, amount of fissile material, and structure of the detector such as moderator, γ-ray shield, thermal neutron shield. Because the detail of the detector design has not been fixed yet, the detection efficiency of the ^{235}U detector is assumed to be 0.07 counts/nv constant for 0.55eV to 2.45MeV, and that of the ^{238}U detector is assumed to be 6×10^{-4} counts/nv constant for neutrons larger than 1MeV.

The toroidal and poloidal cross-sections of the modelling for the MCNP calculation are shown in Fig.5 and Fig.6, respectively. The vacuum vessel has a corrugated structure [9], however, it is modelled to be 4cm thick plate. the poloidal shape of the vacuum vessel is approximated by combined two ellipses. The short radius of inner half ellipse is 1.12m and that of outer half ellipse is 1.27m The poloidal coils are installed so densely inner side of the torus, that those are homogenized in the calculation. The poloidal coils outer side of the torus are modelled truly. The number of the surfaces defining the model is 42. The material and atomic densities of each component are shown in Table 4.

5. RESULTS OF THE CALCULATION

5.1 EXPECTED NEUTRON FLUX AND ENERGY SPECTRUM

Figure 7 shows the neutron flux as a function of major radius on the midplane in the discharge with maximum neutron yield of 2×10^{17} n/s. The fission chambers are planed to be installed around R=5.85m on the midplane, so the neutron flux is expected to be approximately 1×10^{11} n/cm^2 at the detector position in the case of the maximum neutron yield.

The typical neutron energy spectrum expected at detector position is shown in Fig.8. The energy spectrum decreases exponentially to the epithermal region with the decrease of the energy below 0.7MeV. The

the original MCNP code can not treat the toroidal source with the poloidal profile, the distributed source routine for the MORCE code are employed to be linked to the MCNP code. By using the distributed source routine, the plasma parameter dependence of the detection efficiency can be estimated. Standard parameters in the calculation are R_P=3.4m, a_P=0.98m, Z_P=0.16m, κ=1.5, and m=2, which are parameters of the standard divertor configuration.

The lower cut off energy of the calculation is 0.55eV which is a cadmium cutoff energy. The energy bin in the calculation is presented in Table 3. The sensitivities of the detectors to neutrons depend on the fission cross-section, amount of fissile material, and structure of the detector such as moderator, γ-ray shield, thermal neutron shield. Because the detail of the detector design has not been fixed yet, the detection efficiency of the ^{235}U detector is assumed to be 0.07 counts/nv constant for 0.55eV to 2.45MeV, and that of the ^{238}U detector is assumed to be 6×10^{-4} counts/nv constant for neutrons larger than 1MeV.

The toroidal and poloidal cross-sections of the modelling for the MCNP calculation are shown in Fig.5 and Fig.6, respectively. The vacuum vessel has a corrugated structure [9], however, it is modelled to be 4cm thick plate. the poloidal shape of the vacuum vessel is approximated by combined two ellipses. The short radius of inner half ellipse is 1.12m and that of outer half ellipse is 1.27m The poloidal coils are installed so densely inner side of the torus, that those are homogenized in the calculation. The poloidal coils outer side of the torus are modelled truly. The number of the surfaces defining the model is 42. The material and atomic densities of each component are shown in Table 4.

5. RESULTS OF THE CALCULATION

5.1 EXPECTED NEUTRON FLUX AND ENERGY SPECTRUM

Figure 7 shows the neutron flux as a function of major radius on the midplane in the discharge with maximum neutron yield of 2×10^{17} n/s. The fission chambers are planed to be installed around R=5.85m on the midplane, so the neutron flux is expected to be approximately 1×10^{11} n/cm^2 at the detector position in the case of the maximum neutron yield.

The typical neutron energy spectrum expected at detector position is shown in Fig.8. The energy spectrum decreases exponentially to the epithermal region with the decrease of the energy below 0.7MeV. The

intensity of the thermal neutron is unknown because the lower cutoff energy of the calculation is 0.55eV. The average neutron energy is estimated to be 0.8MeV at the detector position.

5.2 SIMULATION OF ONE-POINT CALIBRATION

Figure 9 shows the neutron flux at the detector position whose center is located at at R=5.85m, Z=0.16m and Y=0.15m which is a toroidal shift from the center of the port section as a function of the source position in torus calculated by MCNP with the point source on the magnetic axis. The total neutron flux and fast neutron flux whose energy is 1-2.45MeV are corresponding to the responces of the ^{235}U and ^{238}U detectors, respectively. Neutrons from the region more than 120 degree are shielded by the inside of toroidal coils and the center column. Because the detectors are located 15cm away from the center of the port section, the carves are not symmetry. From the integration of the carves detection efficiencies of the ^{235}U and ^{238}U detectors are estimated to be 3.6×10^{-8} counts/neutron and 9.8×10^{-11} counts/neutron, respectively.

The neutron fluxes at the detector position integrated with toroidal angle from $-\theta$ to $+\theta$ are shown in Fig.10. This figure indicates that more than 90% of the ^{235}U detector counts are contributed by source in the range of θ -85° ~ +85°and more than 90% of the ^{238}U detector counts are contributed by source in the range of θ -70°~+70°. In the one point calibration using neutron source, we should scan the neutron source precisely in the range of θ from -85° to +85°.

5.3 PLASMA PARAMETER DEPENDENCE

The dependence of the m-index which is the power of the parabolic source profile is shown in Figure 11. The error bars represent the statistical errors of Monte Carlo calculation. The efficiency of the ^{235}U detector has a peak around m=4 and one of the ^{238}U detector increases with the increase of m until m=3. The averaged cross-section $\langle\sigma v\rangle$ [16] of the DD reaction is approximately proportional to $Ti^{2.5}$ around Ti=5keV. If the radial profiles of the ion density and ion temperature are parabolic, the source neutron produced by the thermal plasma has a parabolic profile powered by 4.5. However, most of the neutrons in the NB heated plasma are produced by the beam-plasma interactions. So the neuron source profile depends on mainly

the deposition profile of the neutral beam. The m-index is estimated to be approximately 2 in the NB heated discharges. If the typical operational range of the m-index is assumed to be 1 to 3, the uncertainties of the detection efficiencies due to the variation of the m-index are ±7% and ±6% for ^{235}U and ^{238}U detectors, respectively.

Figure 12 shows the ellipticity dependence of the detection efficiencies. Efficiencies increase within the typical operational range of κ 1.3 to 1.7 The uncertainties due to the variation of the ellipticity are ±7% and ±4% for ^{235}U and ^{238}U detectors, respectively, which is smaller than the statitical error of the calculation.

The plasma position dependence of the detection efficiencies are shown in Fig.13 and 14. The efficiencies increase slightly with the increase of R_p. But the efficiencies vary within only ±3% in the typical operational range of R_p. The efficiencies are not sensitive to the horizontal position of the Plasma center around the typical operational range of Z_p.

Figure 15 shows the minor radius dependence of the detection efficiency. The efficiencies decrease with the increase of a_p. The variations are ±3% and ±6% for the ^{235}U and ^{238}U detectors, respectively in the typical operational range of a_p from 0.8m to 1.0m. This figure suggests that one-point calibration using neutron source only on the magnetic axis may over-estimate the detection efficiency about 15%.

5.4 DETECTOR POSITION DEPENDENCE

The detection efficiencies are very sensitive to the major radii of the detector positions as shown in Fig.16. The detector width is too large to regard it as a point detector. The neutron flux is about 20% different between at front side and at back side of the ^{235}U detector. Therefor more precise calculation with modeling of the detector itself is needed.

The vertical position dependence of the detection efficiencies are shown in Fig.17. The efficiency of the ^{235}U detector is not sensitive to the vertical position of the detector in the range Z from -0.3m to 0.5m. The efficiency of the ^{238}U detector has a peak around Z=-0.2m. But the fast neutron flux varies within only 5% in the length of the ^{238}U detector. The efficiencies are not sensitive to horizontal position of the detectors in the typical width of the detectors as shown in Fig. 18.

5.5 TOTAL UNCERTAINTIES OF THE DETECTION EFFICIENCIES

The certainties of the detection efficiencies due to the plasma parameters and the detector positions are summarized in Table 5. Total uncertainties of the detection efficiencies are ±13% and ±9% for ^{235}U and ^{238}U detectors, respectively. The measurement errors of the detectors themselves should be combined to these uncertainties in the actual measurements.

6. DISCUSSION

The fission chambers will be installed in front of the port box as shown in Fig. 3. The port boxes which are made of 2cm thick inconel 625 are not modeled in the calculation. The modelling error of the calculation is seemed to be the results of the neutron streaming from the port box. The streaming effects has been roughly estimated by the calculation of the model with 2cm thick vacuum vessel and without graphite wall, which is a very extreme approximation. The calculated detection efficiencies are shown in Table 6. So the modelling errors of the detection efficiencies are estimated to be not more than 30% and 90% for the ^{235}U and ^{238}U detectors, respectively. The detection efficiency of the ^{238}U detectors is sensitive to the structure in front of the detector because the response of the ^{238}U detector is contributed mainly by direct DD neutrons and one or two times scattered neutrons. The modelling with the port boxes are needed in order to evaluate the detection efficiencies more precisely especially for the ^{238}U detector.

7. CONCLUSION

The neutron source strength of JT-60 Upgrade will be measured with ^{235}U and ^{238}U fission chambers. Detection efficiencies of the fission chambers for the source neutrons are calculated by the Monte Carlo code MCNP with 3-dimensional modelling of JT-60 Upgrade and with poloidally distributed neutron source. More than 90% of the fission chamber's counts are contributed by source of $-85° < \theta < 85°$ in the toroidal angle. The uncertainties of the detection efficiencies due to plasma parameter varieties are ±11% and ±8% for ^{235}U and ^{238}U detectors, respectively. The detection efficiencies are sensitive to the major radius of the detector position, but not so sensitive to vertical and toroidal shift of the detector position. The total uncertainties

5.5 TOTAL UNCERTAINTIES OF THE DETECTION EFFICIENCIES

The certainties of the detection efficiencies due to the plasma parameters and the detector positions are summarized in Table 5. Total uncertainties of the detection efficiencies are ±13% and ±9% for ^{235}U and ^{238}U detectors, respectively. The measurement errors of the detectors themselves should be combined to these uncertainties in the actual measurements.

6. DISCUSSION

The fission chambers will be installed in front of the port box as shown in Fig. 3. The port boxes which are made of 2cm thick inconel 625 are not modeled in the calculation. The modelling error of the calculation is seemed to be the results of the neutron streaming from the port box. The streaming effects has been roughly estimated by the calculation of the model with 2cm thick vacuum vessel and without graphite wall, which is a very extreme approximation. The calculated detection efficiencies are shown in Table 6. So the modelling errors of the detection efficiencies are estimated to be not more than 30% and 90% for the ^{235}U and ^{238}U detectors, respectively. The detection efficiency of the ^{238}U detectors is sensitive to the structure in front of the detector because the response of the ^{238}U detector is contributed mainly by direct DD neutrons and one or two times scattered neutrons. The modelling with the port boxes are needed in order to evaluate the detection efficiencies more precisely especially for the ^{238}U detector.

7. CONCLUSION

The neutron source strength of JT-60 Upgrade will be measured with ^{235}U and ^{238}U fission chambers. Detection efficiencies of the fission chambers for the source neutrons are calculated by the Monte Carlo code MCNP with 3-dimensional modelling of JT-60 Upgrade and with poloidally distributed neutron source. More than 90% of the fission chamber's counts are contributed by source of $-85° < \theta < 85°$ in the toroidal angle. The uncertainties of the detection efficiencies due to plasma parameter varieties are ±11% and ±8% for ^{235}U and ^{238}U detectors, respectively. The detection efficiencies are sensitive to the major radius of the detector position, but not so sensitive to vertical and toroidal shift of the detector position. The total uncertainties

5.5 TOTAL UNCERTAINTIES OF THE DETECTION EFFICIENCIES

The certainties of the detection efficiencies due to the plasma parameters and the detector positions are summarized in Table 5. Total uncertainties of the detection efficiencies are ±13% and ±9% for ^{235}U and ^{238}U detectors, respectively. The measurement errors of the detectors themselves should be combined to these uncertainties in the actual measurements.

6. DISCUSSION

The fission chambers will be installed in front of the port box as shown in Fig. 3. The port boxes which are made of 2cm thick inconel 625 are not modeled in the calculation. The modelling error of the calculation is seemed to be the results of the neutron streaming from the port box. The streaming effects has been roughly estimated by the calculation of the model with 2cm thick vacuum vessel and without graphite wall, which is a very extreme approximation. The calculated detection efficiencies are shown in Table 6. So the modelling errors of the detection efficiencies are estimated to be not more than 30% and 90% for the ^{235}U and ^{238}U detectors, respectively. The detection efficiency of the ^{238}U detectors is sensitive to the structure in front of the detector because the response of the ^{238}U detector is contributed mainly by direct DD neutrons and one or two times scattered neutrons. The modelling with the port boxes are needed in order to evaluate the detection efficiencies more precisely especially for the ^{238}U detector.

7. CONCLUSION

The neutron source strength of JT-60 Upgrade will be measured with ^{235}U and ^{238}U fission chambers. Detection efficiencies of the fission chambers for the source neutrons are calculated by the Monte Carlo code MCNP with 3-dimensional modelling of JT-60 Upgrade and with poloidally distributed neutron source. More than 90% of the fission chamber's counts are contributed by source of $-85° < \theta < 85°$ in the toroidal angle. The uncertainties of the detection efficiencies due to plasma parameter varieties are ±11% and ±8% for ^{235}U and ^{238}U detectors, respectively. The detection efficiencies are sensitive to the major radius of the detector position, but not so sensitive to vertical and toroidal shift of the detector position. The total uncertainties

combined detector position errors are ±13% and ±9% for ^{235}U and ^{238}U detectors, respectively. The modelling errors of the detection efficiencies are so large especially for the ^{238}U detector that the modelling with the port boxes are needed

ACKNOWLEDGEMENTS

The author would like to thank Drs K. Nagashima, Y. Kusama, H. Takeuchi, and S. Seki for their fruitful discussions. The continuing supports of Drs. M. Yoshikawa, S. Tamura, and A. Funahashi are gratefully acknowledged.

combined detector position errors are ±13% and ±9% for ^{235}U and ^{238}U detectors, respectively. The modelling errors of the detection efficiencies are so large especially for the ^{238}U detector that the modelling with the port boxes are needed

ACKNOWLEDGEMENTS

The author would like to thank Drs K. Nagashima, Y. Kusama, H. Takeuchi, and S. Seki for their fruitful discussions. The continuing supports of Drs. M. Yoshikawa, S. Tamura, and A. Funahashi are gratefully acknowledged.

REFERENCES

[1] E. B. Nieschmidt, A. C. England, H.W. Hendel, J. A. Isaacson, L. P. Ku, F. Y. Tsang, Rev. Sci. Instrum. **56** (1985) 1084

[2] H. W. Hendel, D. L. Jassby, H. S. Bosch, Cris. W. Barnes, L. C. Johnson, T. J. Murphy, E. B. Nieschmidt, T. Saito,J. D. Strachan, G. D. Tait,K. M. Young, Rev. Sci. Instrum. **59** (1988) 1682

[3] E. B. Nieschmidt, T. Saito, C. W. Barnes, H.-S. Bosch, T. J. Murphy, Rev. Sci. Instrum. **59** (1988) 1715

[4] H.-S. Bosch, J. D. Strachan, Cris W. Barnes, E. B. Nieschmidt, Rev. Sci. Instrum. **59** (1988) 1718

[5] O. N. Jarvis, J. Källne, G. Sadler, P. van Belle, K. H. Beimer, T. Elevant, A. R. Talbot, JET Report, JET-IR(84)02 (1984)

[6] O. N. Jarvis, J. Källne, G. Sadler, P. van Belle, M Hone, M. Merlo, E. W. Lees, M. T. Swinhoe, A. R. Talbot, A. H. Armitage, JET Report, JET-IR(85)06(1984)

[7] G. Zankel, J. D. Strachan, R.Lewis, W. Pettus, J. Schmotzer, Nucl. Instrum. Methods **185** (1981) 321

[8] K. Hübner,et al., in 16th Europ. Conf. on Controlled Fusion and Physics, (Venice,1989) part 4, p1453

[9] M. Kikuchi, T. Ando, M. Araki, T. Horie, H. Horiike, Y. Ikeda, H. Kishimoto, K. Koizumi, M. Matsukawa, T. Matsukawa, Y. Neyatani, H. Ninomiya, T. Nishitani, S. Seki, H. Takatsu, M. Yamamoto, in Symp. on Fusion Technol. 1988, 9Utrecht, 1988) p287

[10] "MCNP MonteCarlo Neutron and Photon Transport Code", Ork Ridge National Laboratory, CCC-200 (1983)

[11] B. L. Kirk, J. T. West, Ork Ridge National Laboratory Report, ORNL/TM-9123 (1984)

[12] T. Nishitani, J. D. Strachan, Princeton Plasma Physics Laboratory Report, PPPL-2512 (1988)

[13] J. D. Strachan, T. Nishitani, Cris W. Barnes, Rev. Sci. Instrum. **59** (1988) 1732

[14] V. V. Verbinski, W. R. Burrus. T. A. Love, W. Zobel. N. W. Hill, R. Textor, Nucl. Instrum. Methods **65** (1968) 8

[15] A. C. England, H. W. Hendel, E. B. Nieschmidt, Rev. Sci. Instrum. **57** (1986) 1754

[16] H. P. Eubank, "Diagnostics for Fusion Experiments", Varenna,1978 , Pergamon Press

Table 1 Machine and plasma parameters of JT-60 Upgrade.

Machine Parameters	
Major Radius	3.4 m
Minor Radius	1.1 m
Elongation	1.4-1.7
Toroidal Field	4.2 T
Plasma Current	6MA(Divertor), 7 MA(Limiter)
Discharge Duration	15 sec
Operational gas	Deuterium
Heating Power (Torus Input)	40 MW(NBI)
	15 MW(LHRF)
	10 MW(ICRF)
Expected Plasma Parameters	
τ_E	0.6-1.2 sec
$n_{e(0)}$	$1\text{-}10\times10^{19}$ m^{-3}
$T_{i(0)}$	10-20 keV
$n_i(0)T_i(0)t_E$	$\sim0.5\times10^{21}$ $keVm^{-3}sec$
Maximum neutron yield	2×10^{17} n/s

Table 2 Neutron diagnostics plan on JT-60 Upgrade.

Diagnostics	Specification
Fission chambers	^{235}U&^{238}U, 3 point, Δt=1-10ms
^{3}He ion chamber spectrometer	1point, ΔE~2%
NE213 scintiration detector	1point, ΔE~10%
Activation foil method	1~3point, no time resolution
Neutron multicollimator (proposed)	10point, Δt=1-10ms

Table 3 Energy grops in the MCNP calculations.

Group No.	Energy range (eV)		
1	2.23×10^{6}	~	2.74×10^{6}
2	1.23×10^{6}	~	2.23×10^{6}
3	8.21×10^{5}	~	1.23×10^{6}
4	4.51×10^{5}	~	8.21×10^{5}
5	2.73×10^{5}	~	4.51×10^{5}
6	1.66×10^{5}	~	2.73×10^{5}
7	6.74×10^{4}	~	1.66×10^{5}
8	1.93×10^{4}	~	6.74×10^{4}
9	2.61×10^{3}	~	1.93×10^{4}
10	3.54×10^{2}	~	2.61×10^{3}
11	4.79×10^{1}	~	3.54×10^{2}
12	3.93×10^{0}	~	4.79×10^{1}
13	0.55×10^{0}	~	3.93×10^{0}

Table 4 Atomic densities of the components in the MCNP calculations.

Atom	Atomic density ($\times 10^{24}$ atoms/cm^3)					
	high manganee steel	inconel 625	graphite	TFC	PFC	PFC homoginized
^{12}C		2.106E-4	8.724E-2			
^{27}Al		3.750E-4				
Si		4.504E-4				
Cr	4.576E-3	2.113E-2		7.894E-4		
Mn	1.559E-2	2.302E-4		2.689E-3		
Fe	6.561E-2	2.265E-3		1.132E-2		
Ni		5.256E-2				
Cu				7.012E-2	8.474E-2	1.338E-2
Ni		6.716E-3				

Table 5 Uncertainties of the detection efficiencies owing to plasma parameter variation and the neutron flux variation in the detector size.

	^{235}U Detector	^{238}U Detector
Plasma Parameters	±11%	±8%
m-index	±7%	±6%
κ	±7%	±3%
R_P	±3%	±2%
Z_P	±3%	±2%
a_P	±2%	±4%
Detector Position	±7%	±4%
R	±5%	±3%
Z	±2%	±1%
Y	±2%	±2%
Total Uncertainty	±13%	±9%

Table 6 Detection efficiencies for the full model and the model without graphite wall and with the half thick vacuum vessel.

Modelling	^{235}U Detector	^{238}U Detector
Full Modelling	3.4×10^{-8}	8.5×10^{-11}
No Graphite Wall and Half Thick Vacuum Vessel	4.4×10^{-8}	1.6×10^{-10}

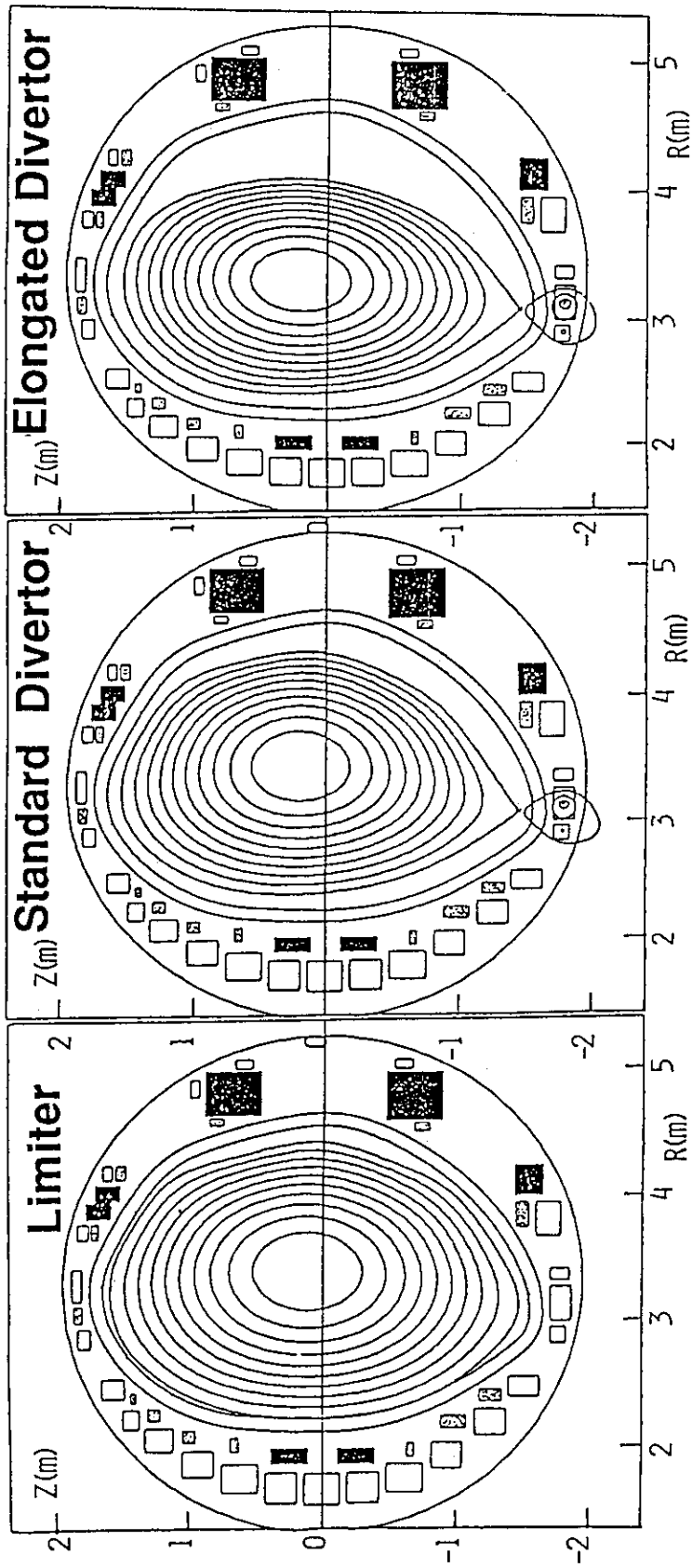

Fig. 1 Typical magnetic configurations of JT-60 Upgrade.

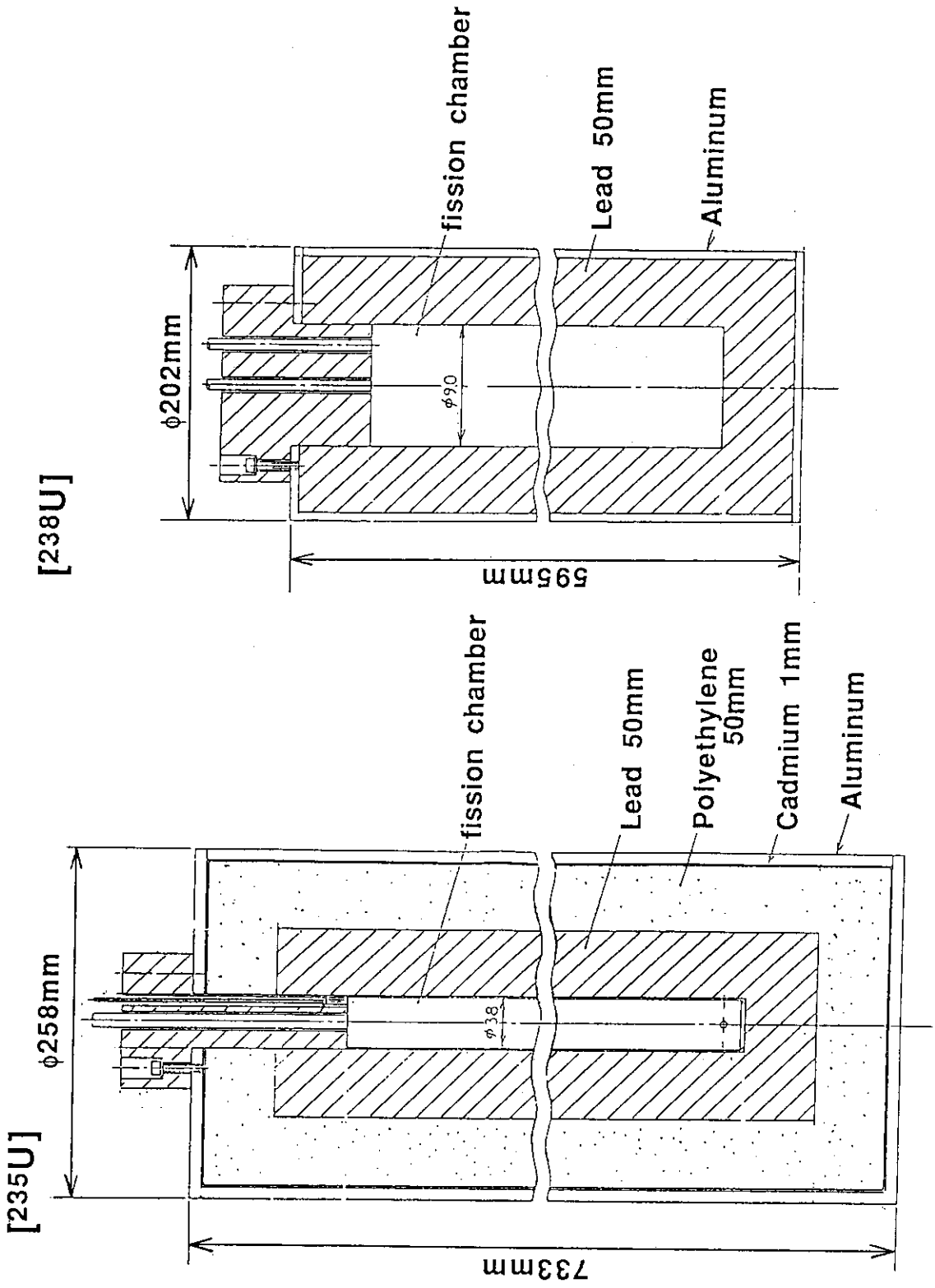

Fig. 2 Schematic diagrams of .fission chambers and assemlies suggested for neutron source strength measurement.

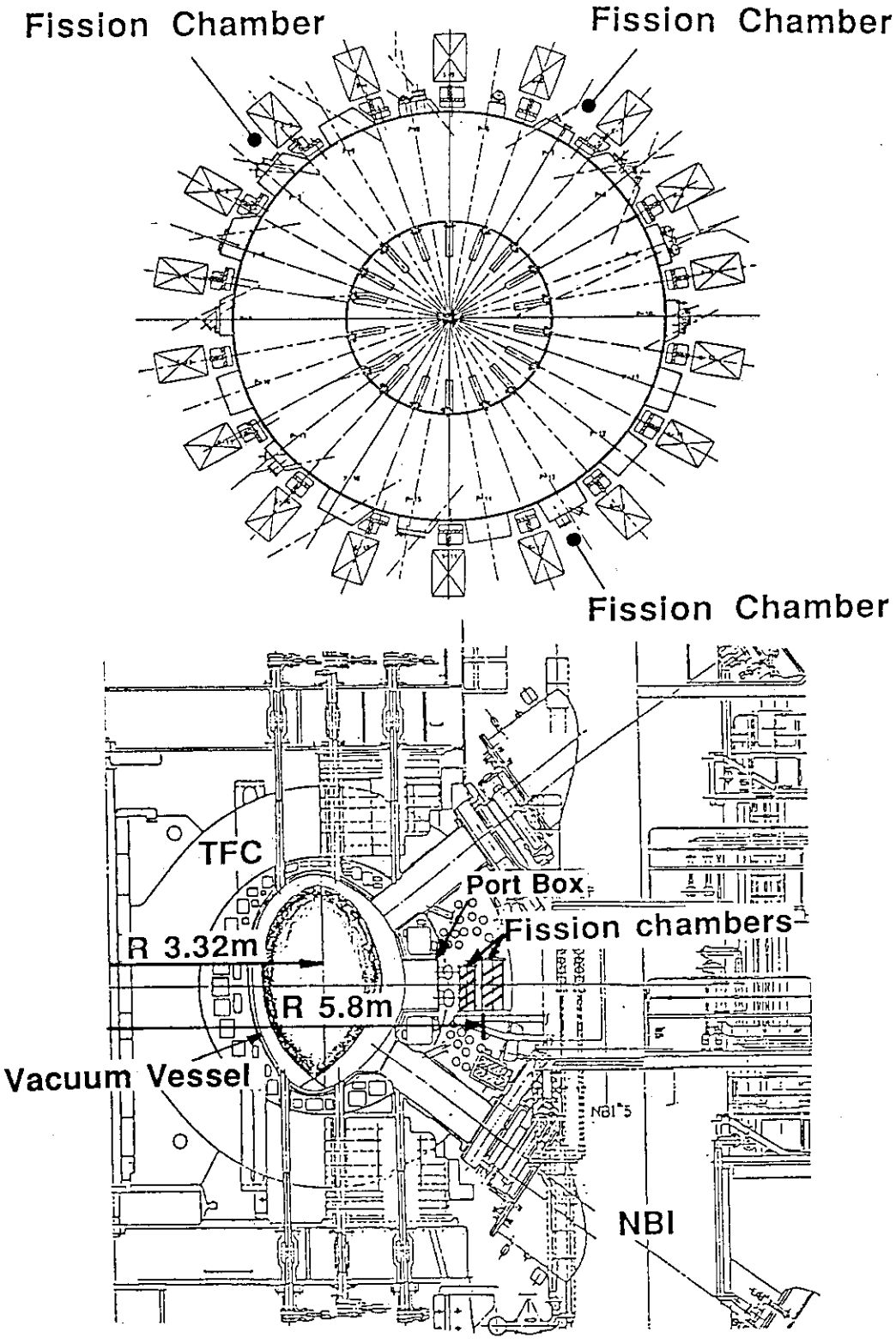

Fig. 3 Arrangement of the detectors on JT-60 Upgrade.

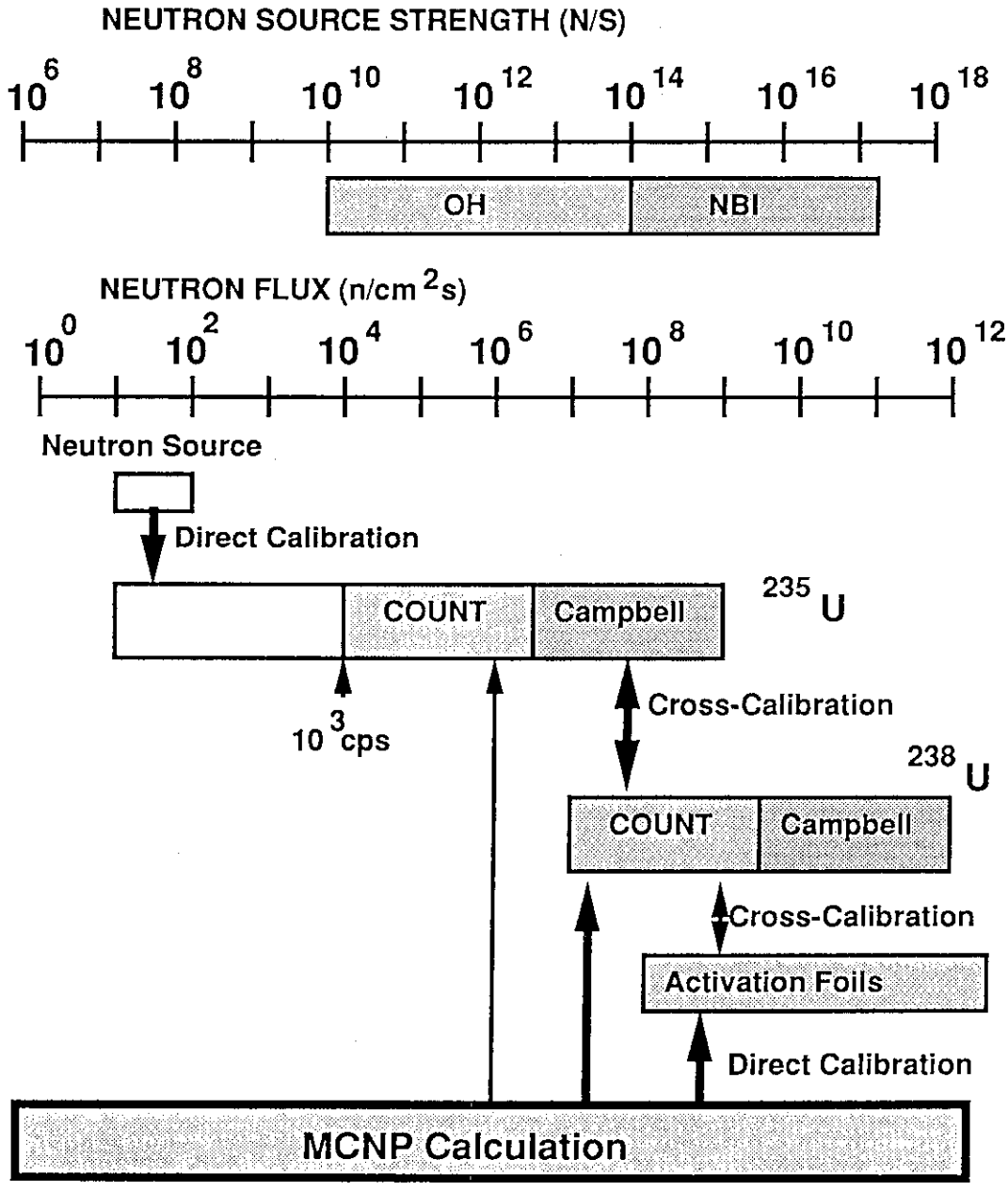

Fig. 4 Diagram of the neutron calibration plan on JT-60 Upgrade.

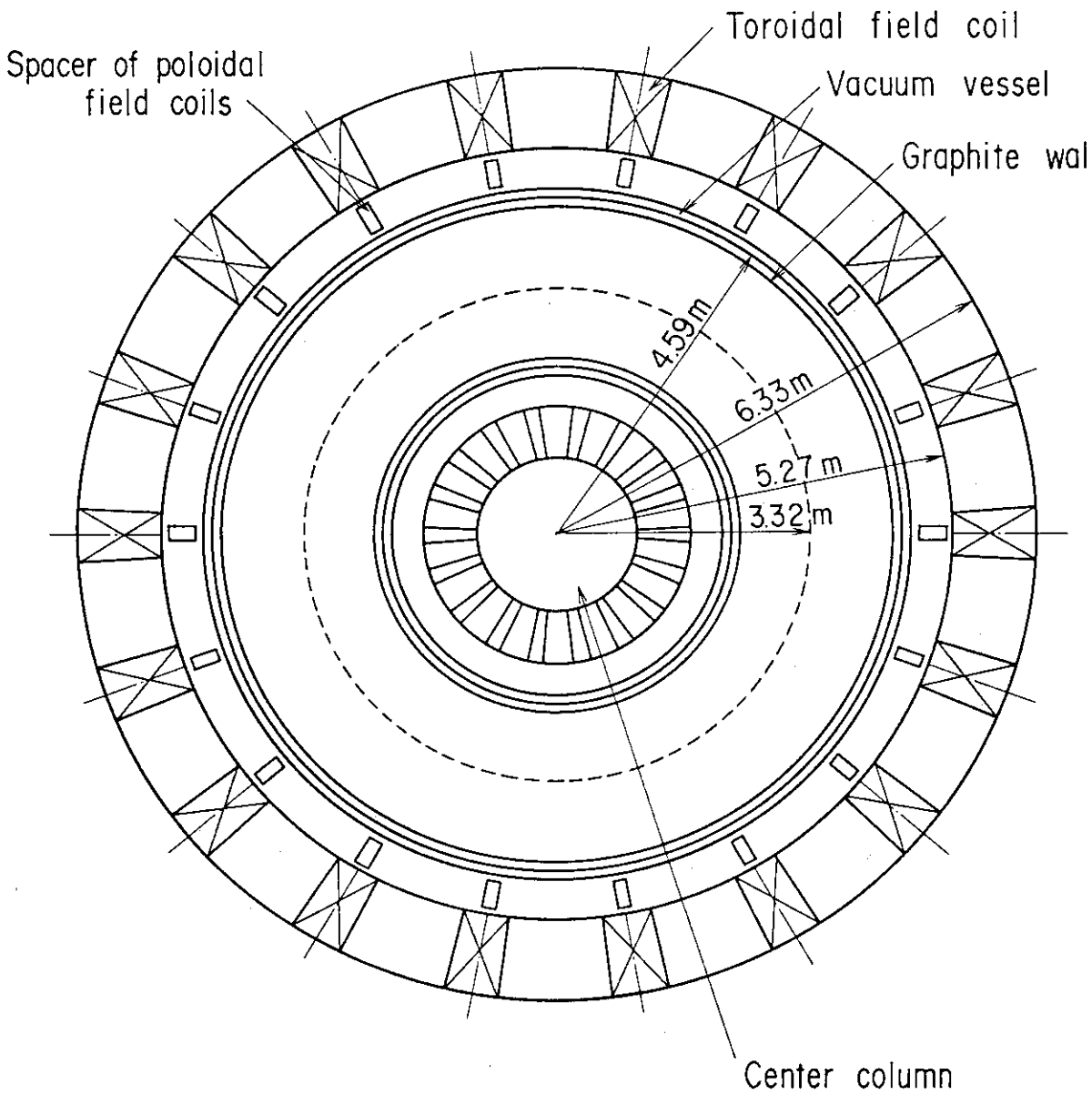

Fig. 5 Toroidal cross-section of the calculation model for JT-60 Upgrade.

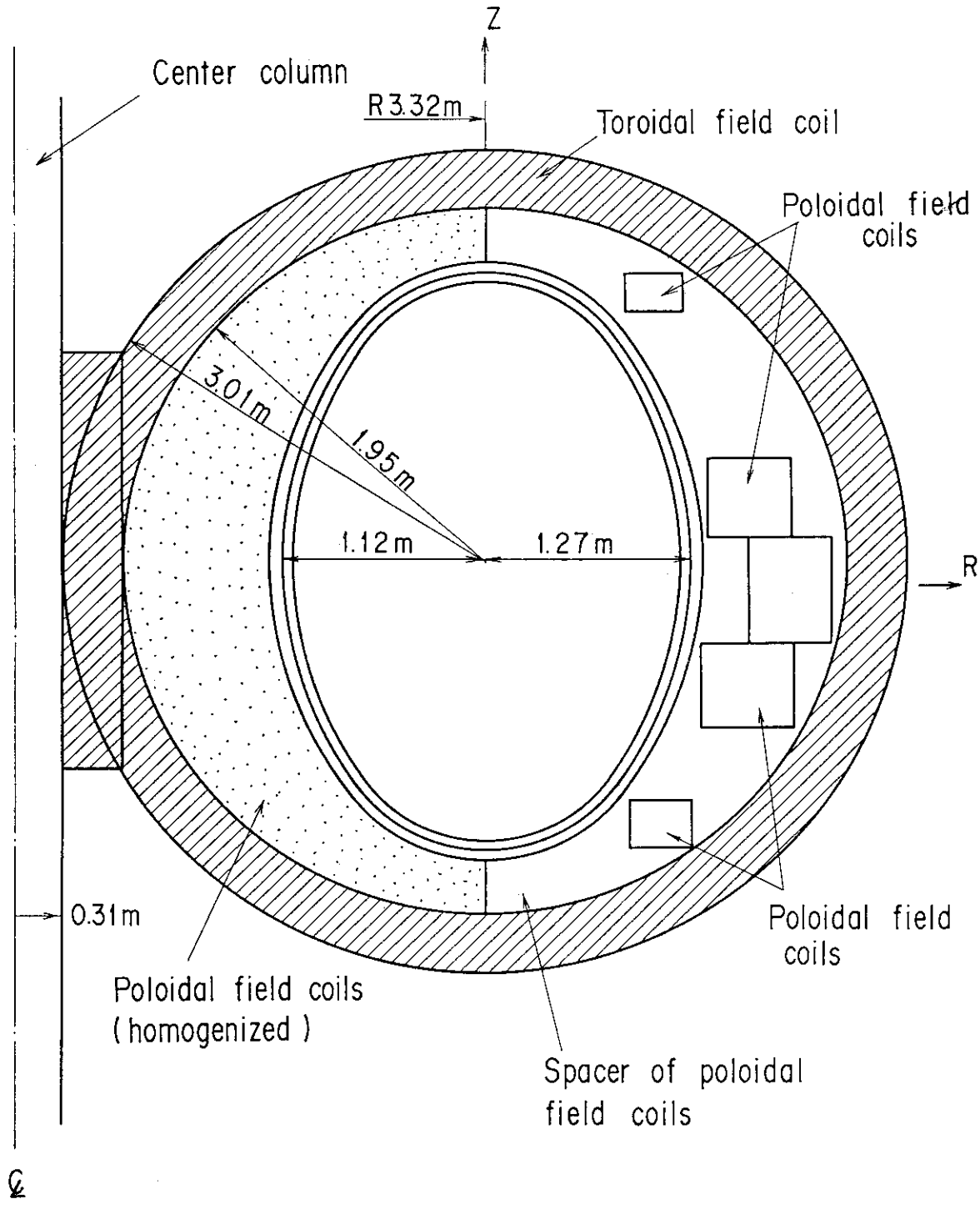

Fig. 6 Poloidal cross-section of the calculation model for JT-60 Upgrade.

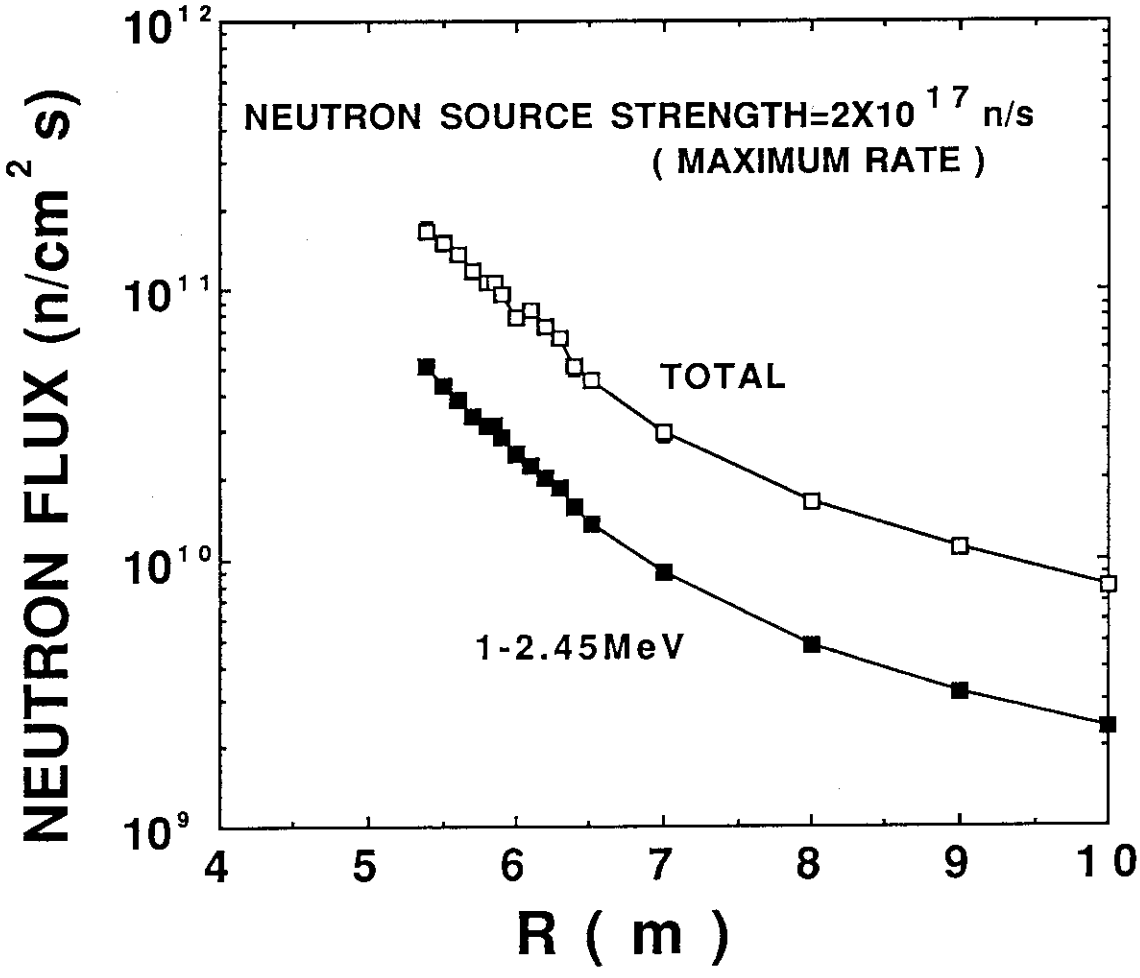

Fig. 7 Total and fast neutron fluxes as a function of major radius on the midplane in the discharge with maximum neutron yield of 2×10^{17} n/s.

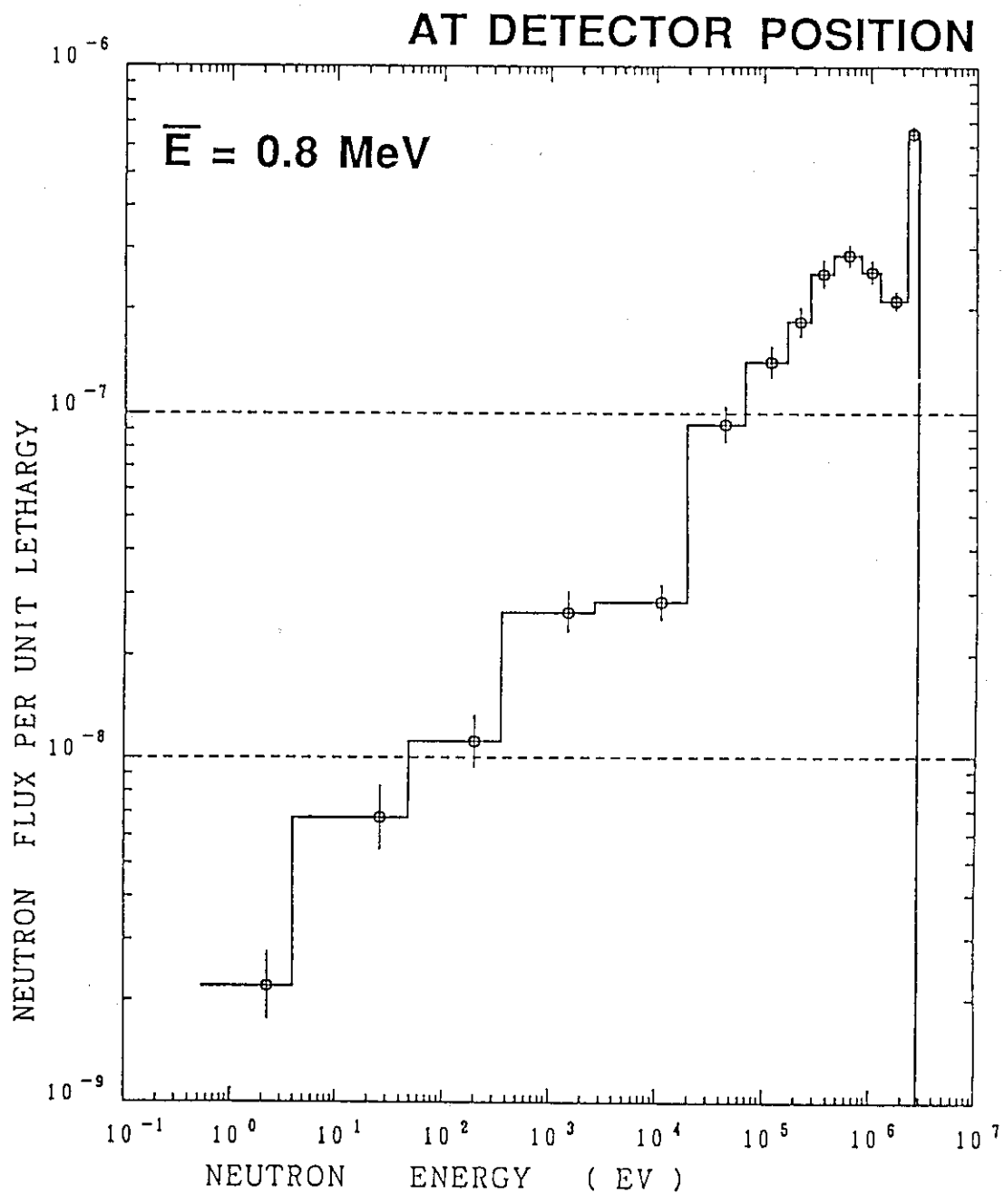

Fig. 8 Typical neutron energy spectrum expected at detector position.

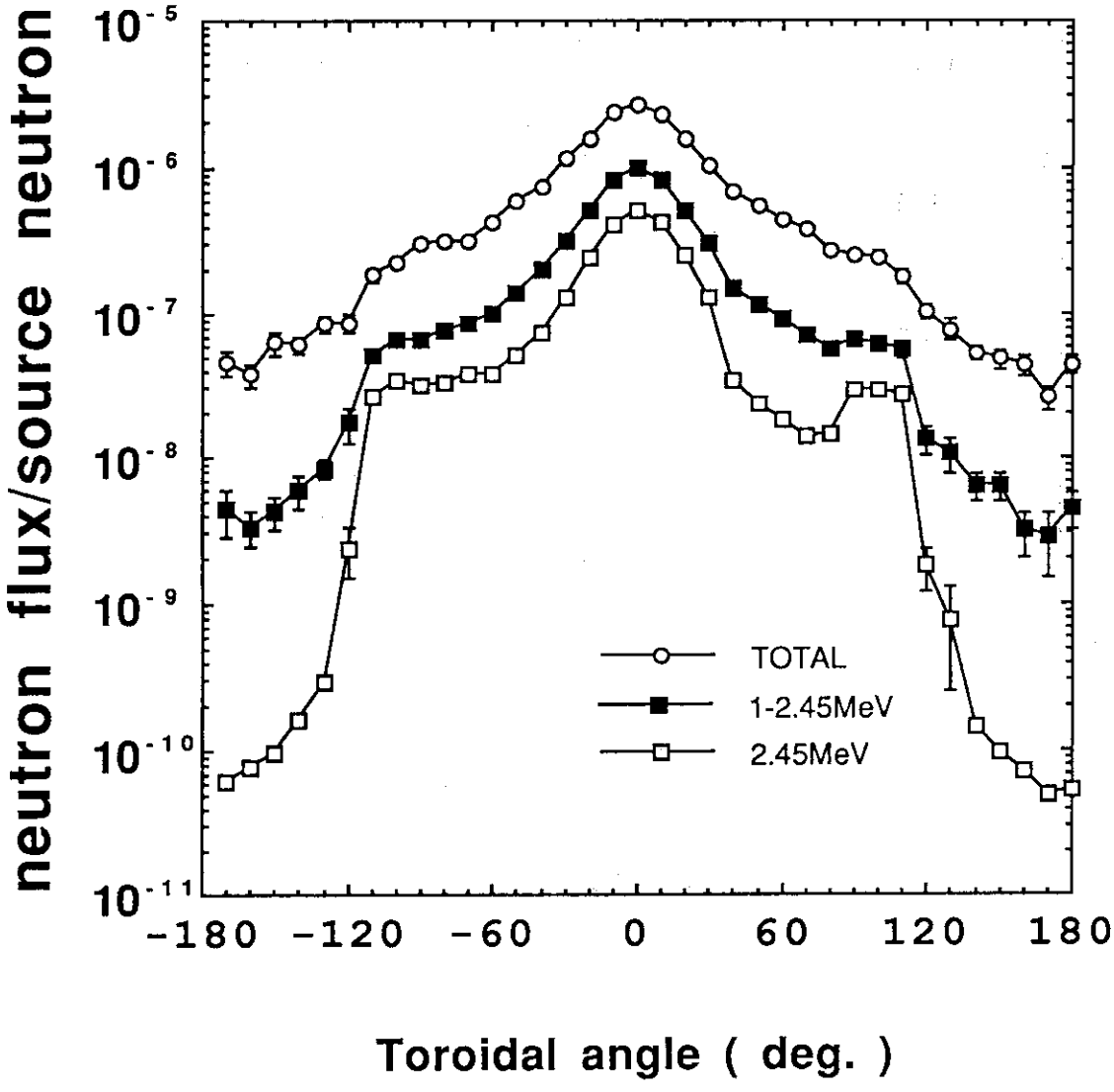

Fig. 9 Neutron flux at the detector position as a function of the source position in the torus calculated by MCNP with the point source on the magnetic axis.

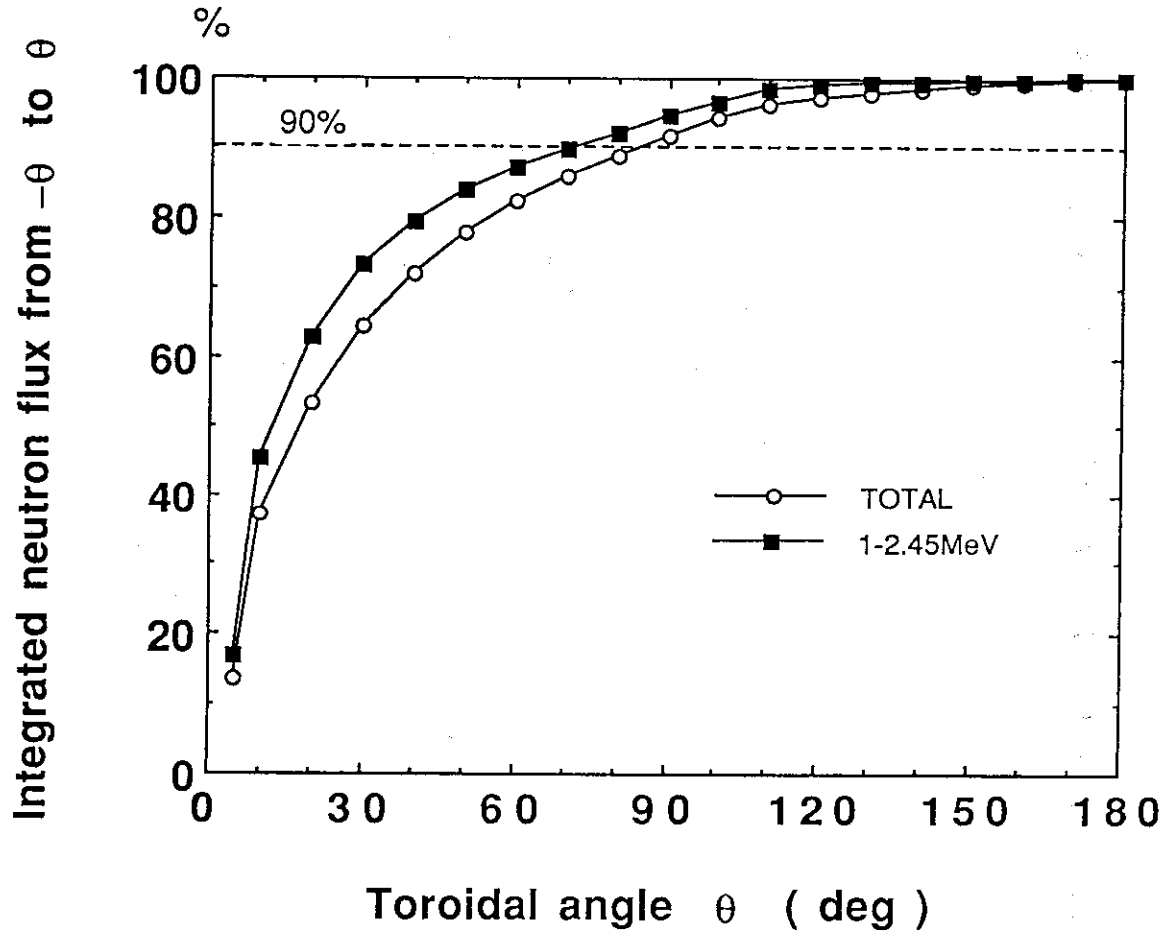

Fig. 10 Neutron fluxes at the detector position integrated with toroidal angle from -θ to +θ.

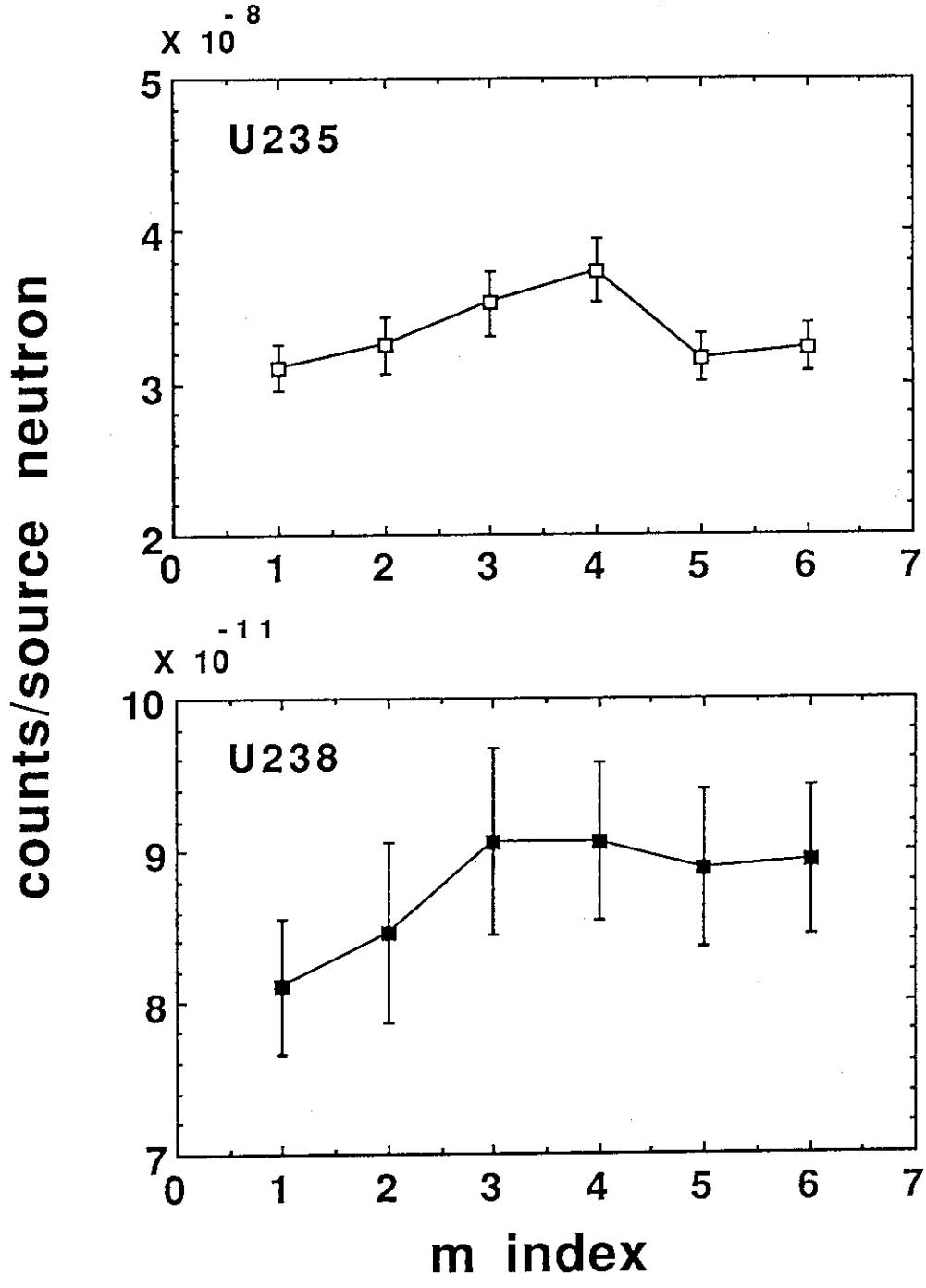

Fig. 11 The m-indexdependence of the detection efficiencies, where m-index is the power of the parabolic source profile.

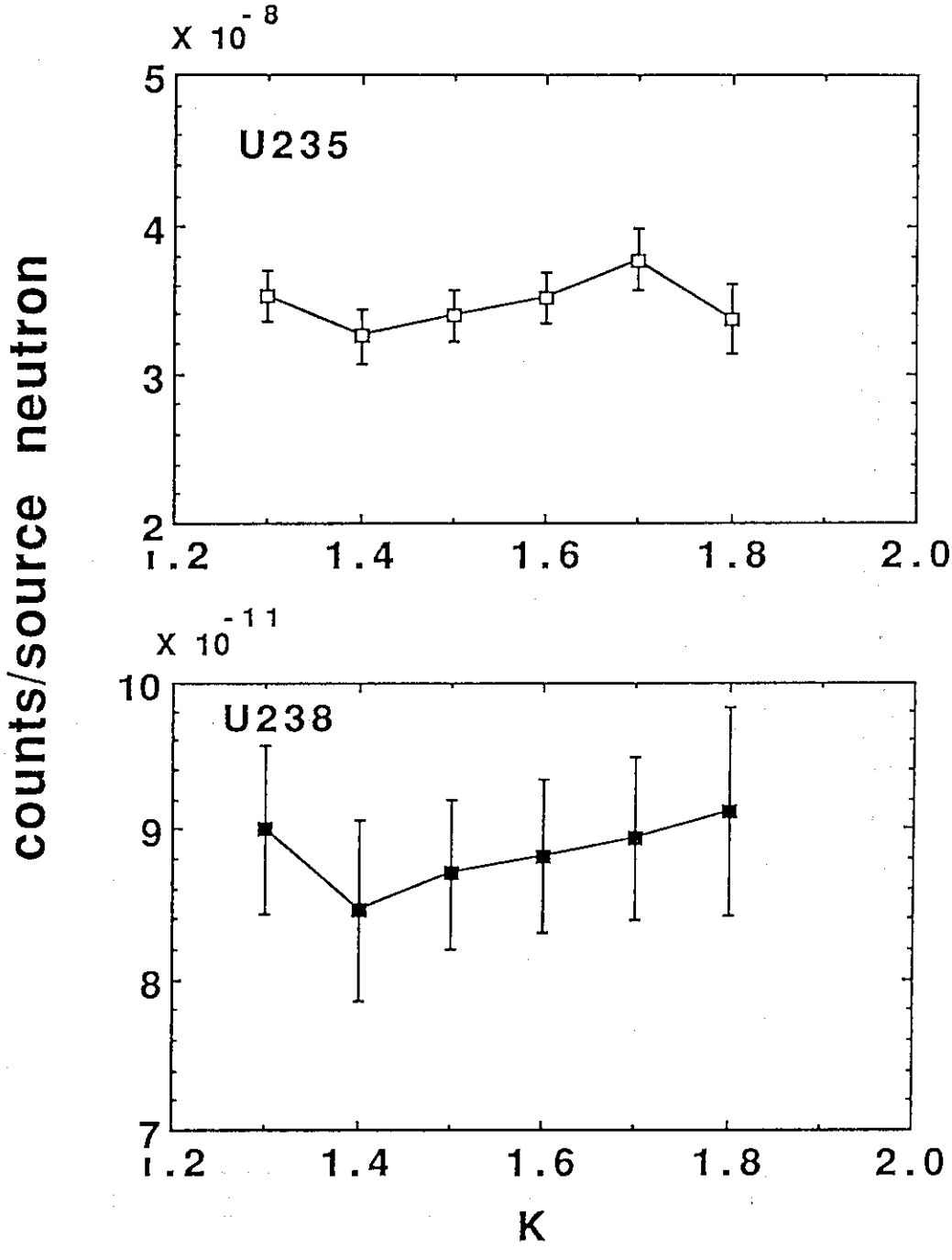

Fig. 12 Ellipticity dependence of the detection efficiencies.

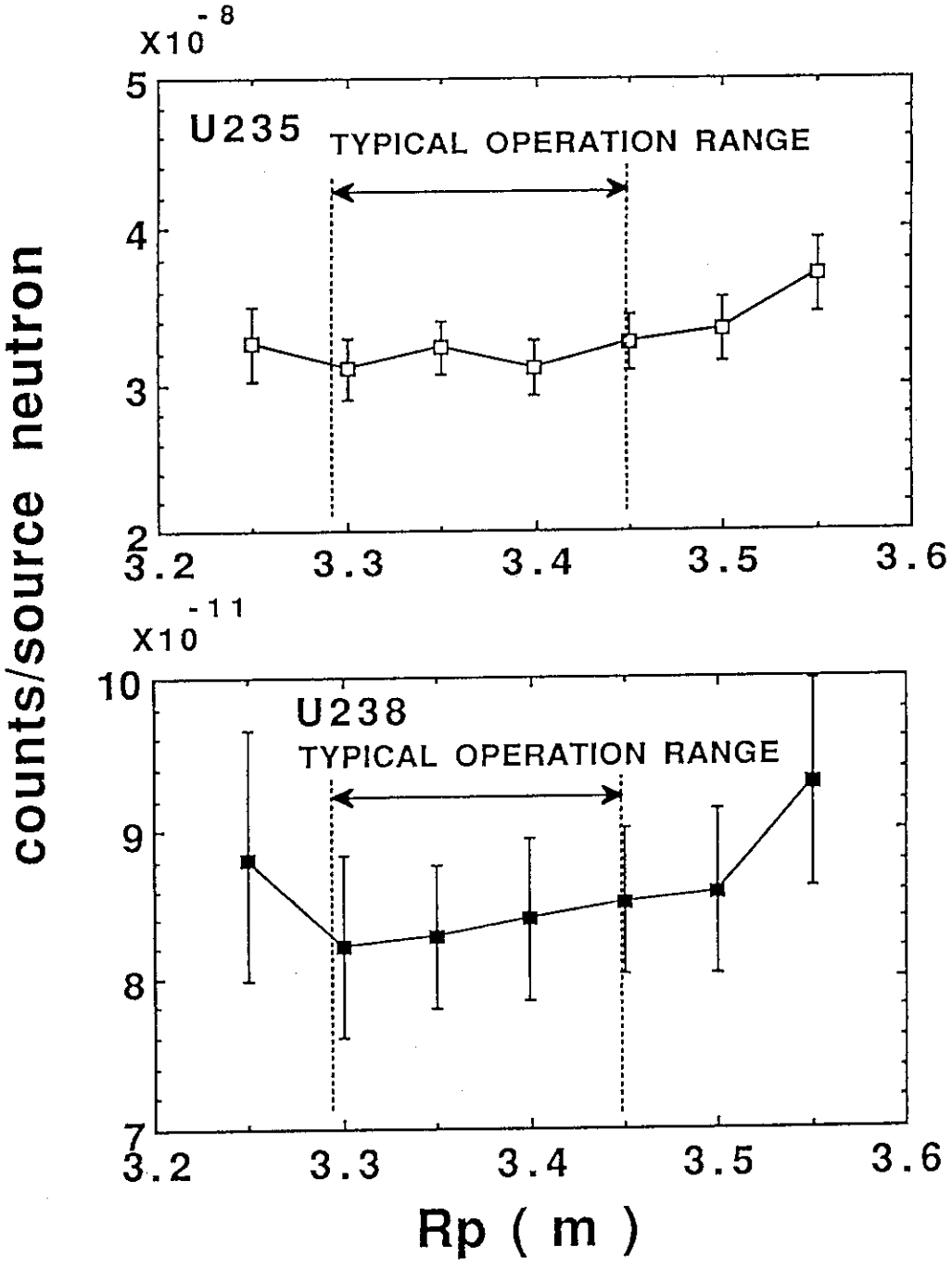

Fig. 13 Radial plasma position dependence of the detection efficiencies.

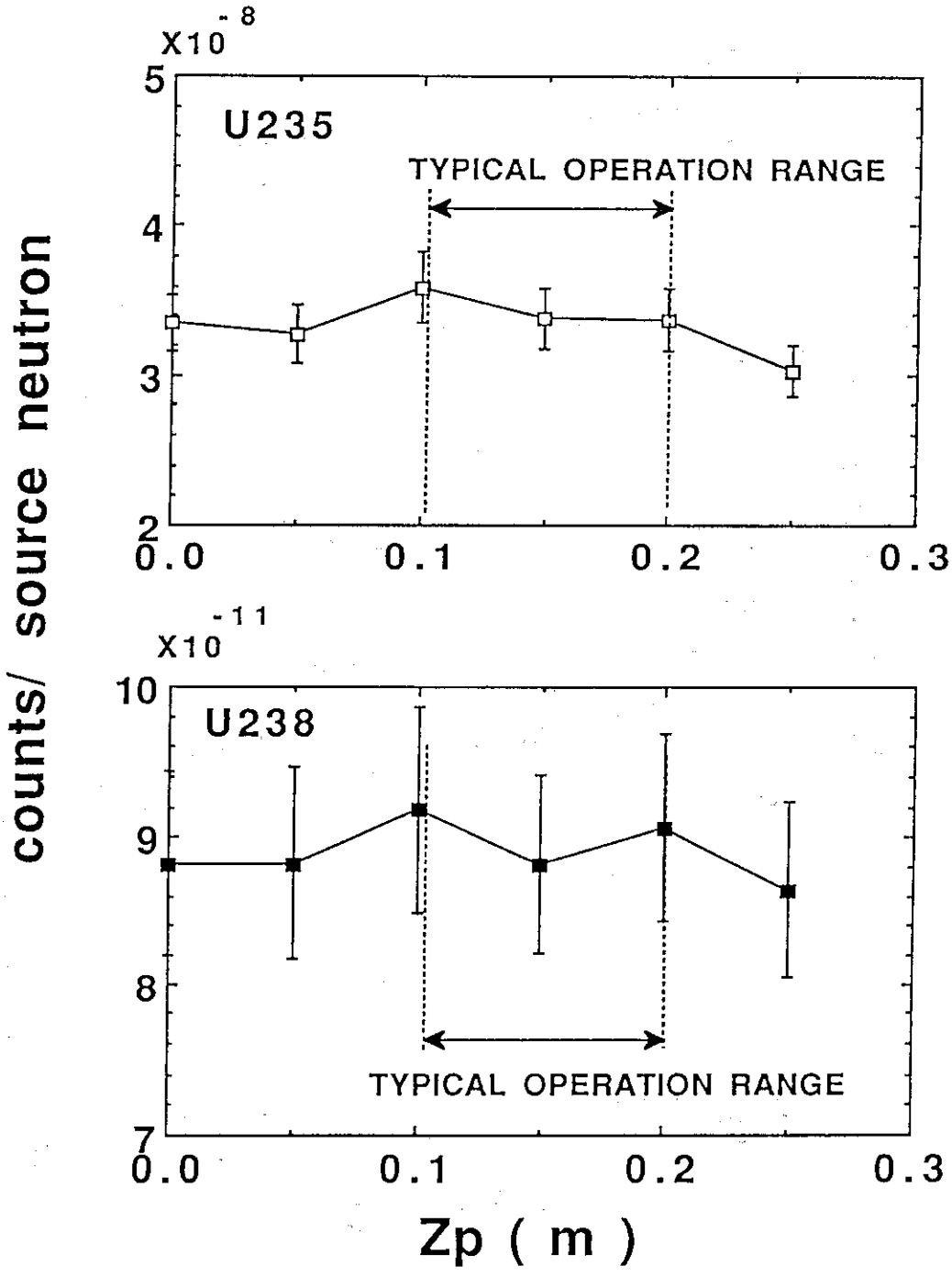

Fig. 14 Vertical plasma position dependence of the detection efficiencies.

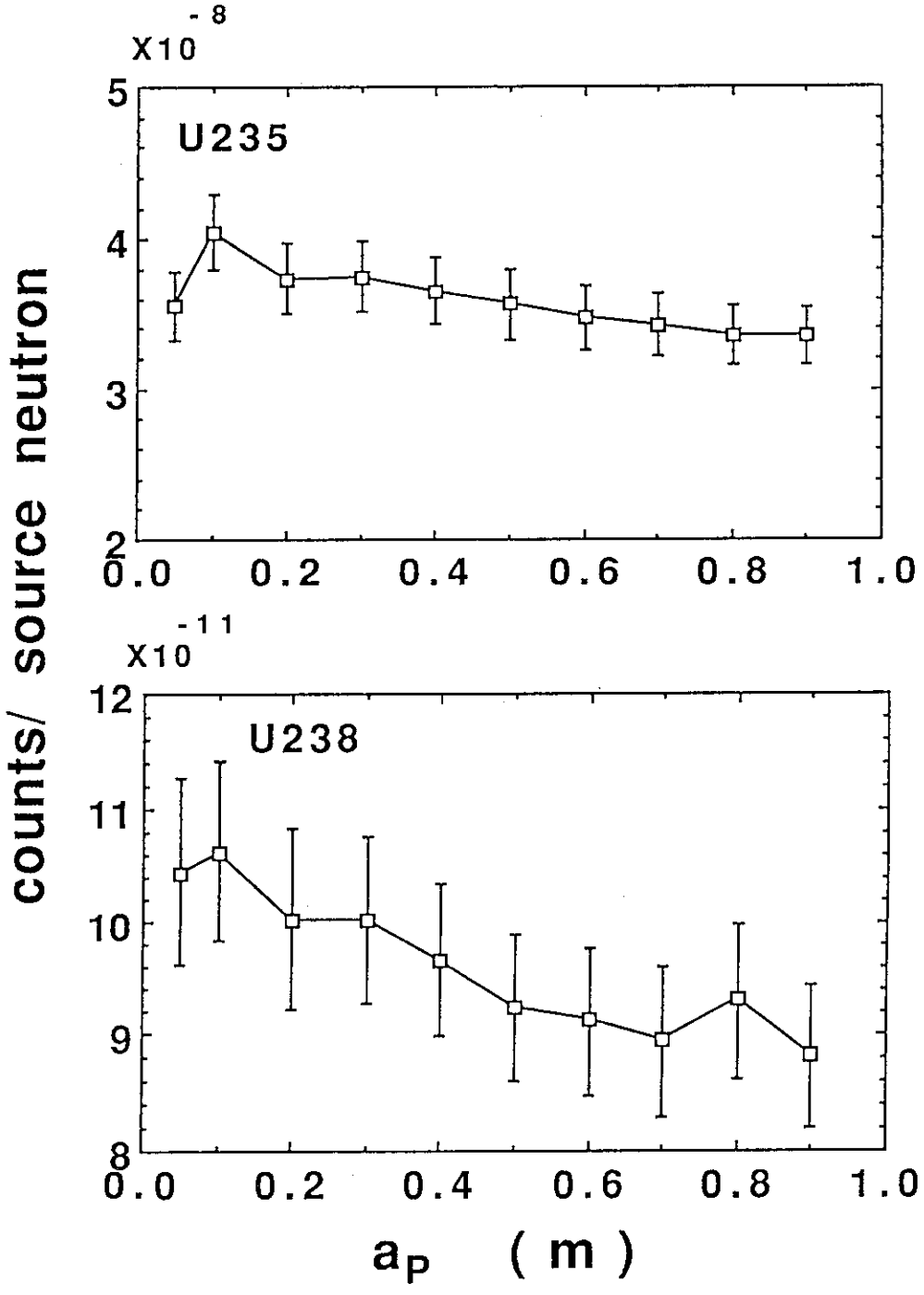

Fig. 15 Plasma minor radius dependence of the detection efficiencies.

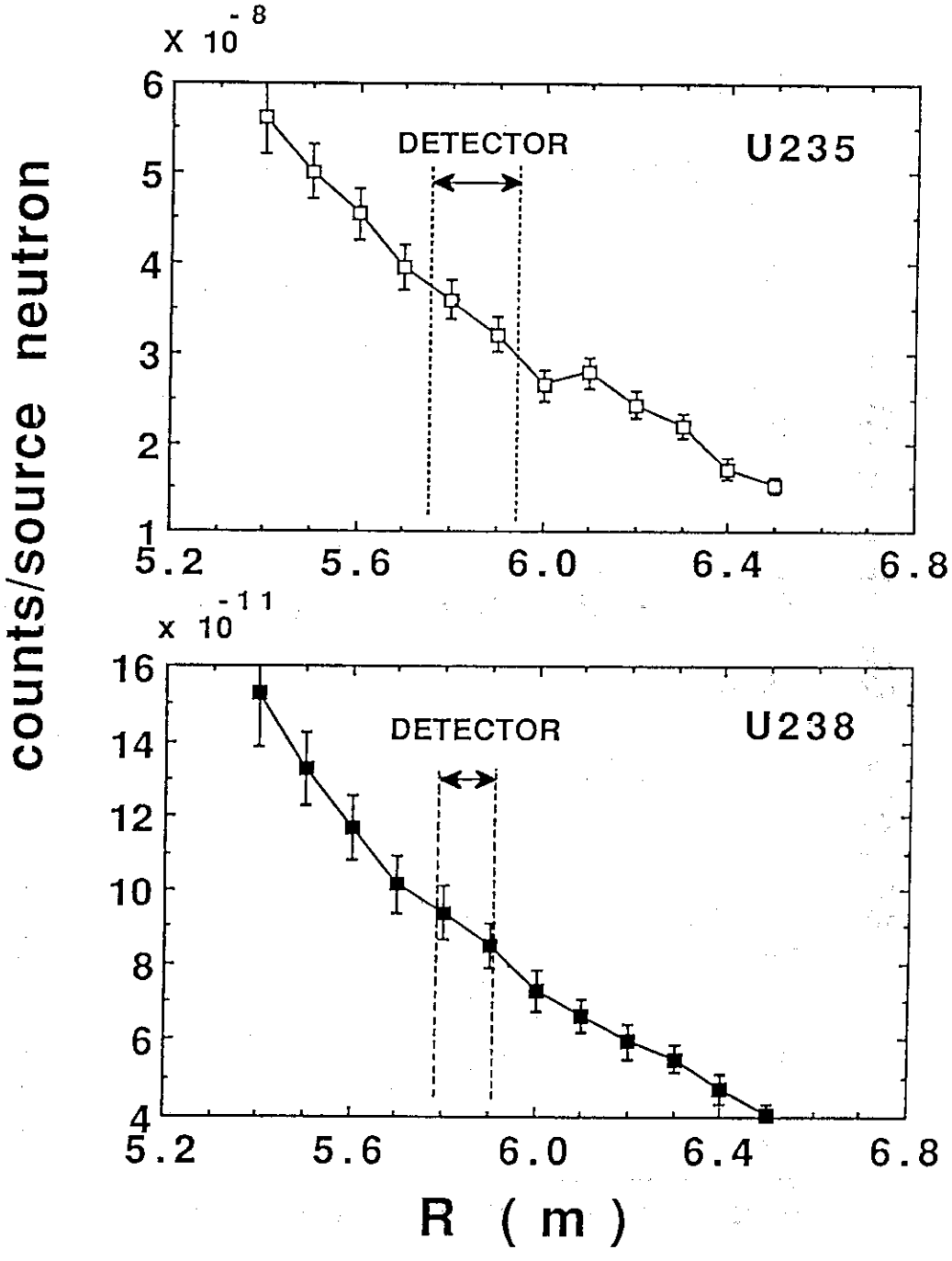

Fig. 16 Detector position dependence of the detection efficiencies in radial direction.

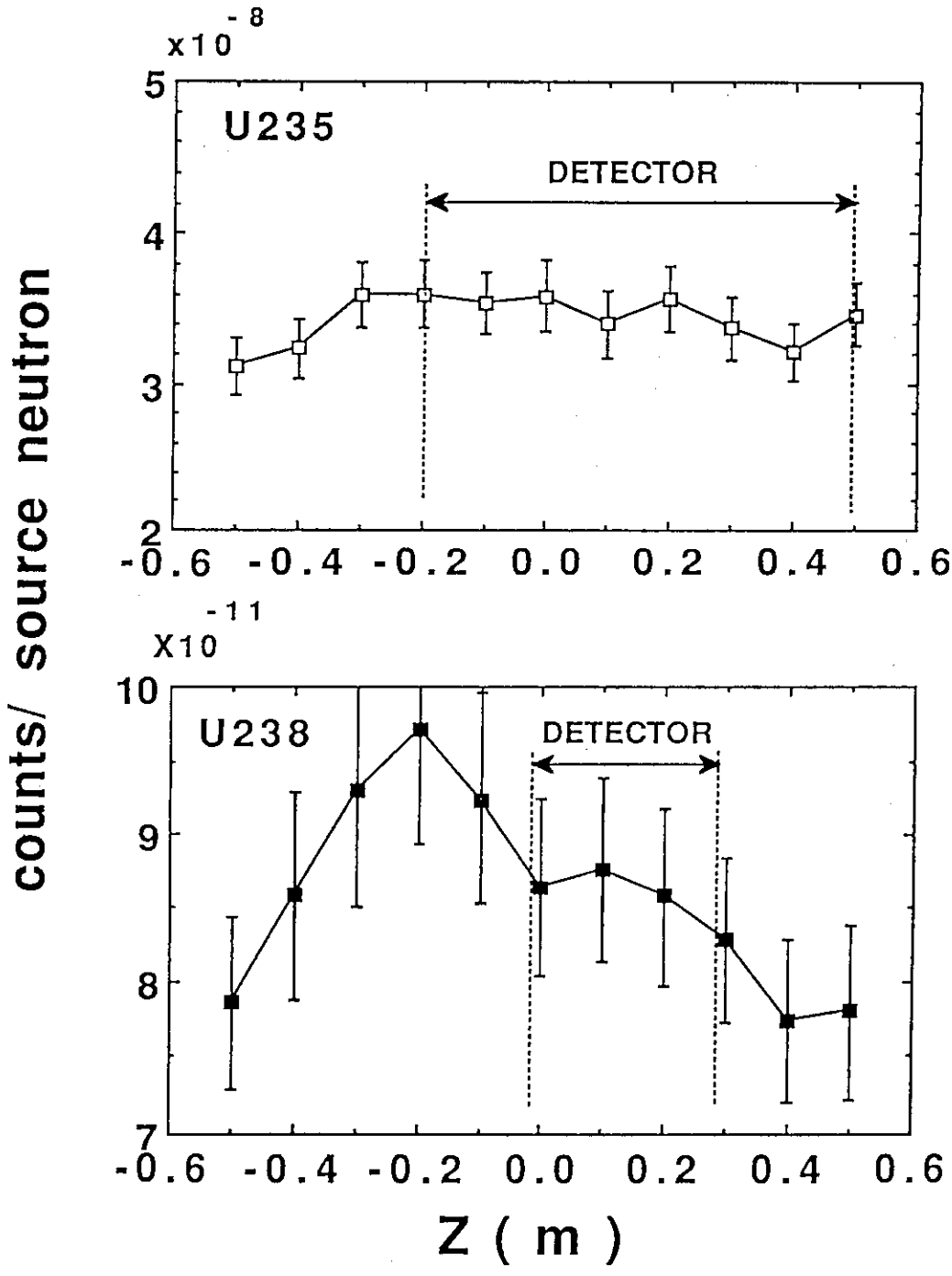

Fig. 17 Detector position dependence of the detection efficiencies in vertical direction.

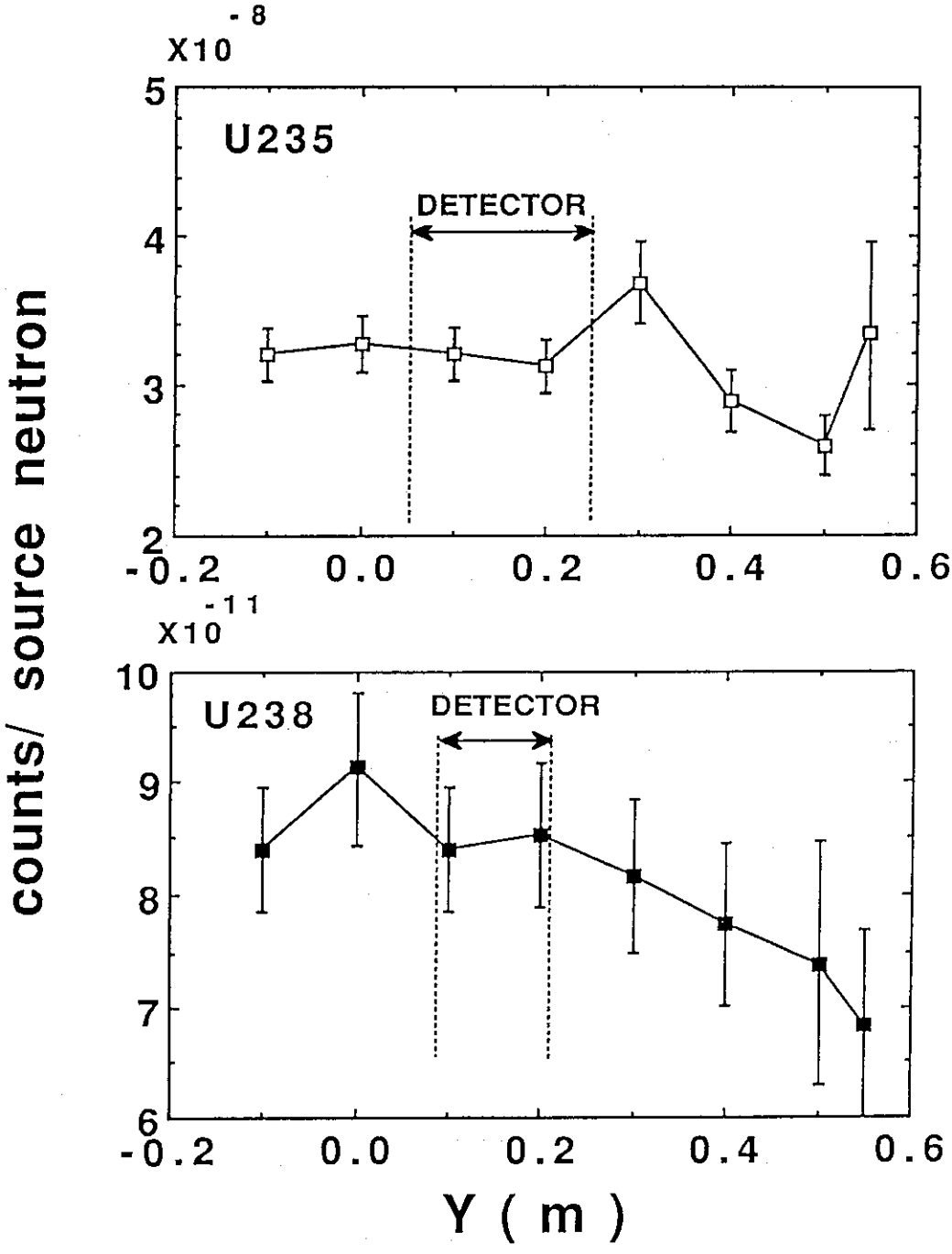

Fig. 18 Detector position dependence of the detection efficiencies in toroidal direction.